Large-scale structure as a critical phenomenon

Zygmunt Lalak and Burt A. Ovrut
Department of Physics, University of Pennsylvania, Philadelphia, Pennsylvania 19104-6396

Steven Thomas
Theory Division, CERN, 1211 Geneva 23, Switzerland
(Received 23 July 1992; revised manuscript received 8 December 1994)

We present an analytical theory for the spatial distribution of energetically soft domain walls produced in cosmological phase transitions. It is shown that this distribution is well described by statistical percolation theory where the probability parameter p is smaller than the critical probability p_c. We discuss, in detail, the nonequilibrium phase transition that triggers the formation of domain walls. We then briefly describe two applications of these ideas, the first to the formation of the Abell clusters and voids and the second to the energy density fluctuations generated during a generic predecoupling phase transition.

PACS number(s): 98.80.Cq, 05.70.Jk

I. INTRODUCTION

It has long been known [1,2] that there is substantial clustering of galaxies on length scales of the order of 1 Mpc. More recently, it has become clear [3] that there are large voids, walls of galaxies, and gravitational attractors on scales of the order of 50 Mpc. All this large-scale structure occurs at relatively recent times, with redshifts $z < 10$. It is not impossible that this structure occurs solely as a consequence of the gravitational accretion of matter to density perturbations arising from processes in the very early Universe, such as inflation [4]. However, it has not been established that the distinct clustering of galaxies that is observed arises in this manner. In fact, preliminary findings seem to imply that it is very difficult to account simultaneously for the observed clustering at both small and large scales in this way. Other, very different, mechanisms have been postulated to account for large-scale structure. These include gravitational accretion of matter to topological structures such as domain walls [5], cosmic strings [6], and textures [7]. Many of these attempts lead to serious conflict with observation, while others remain viable. In an attempt to overcome some of the difficulties with these mechanisms, a number of authors [8] discussed the possibility of a "late-time" phase transition in a scalar field. This phase transition would produce domain walls at very small z, which would act as the seeds for the formation of the large-scale structure without large, unobserved distortions in the cosmic microwave background. However, it was shown in [9] that these theories apparently lead to large relativistic walls which are in conflict with observation. In addition, the original theories of late-time transitions are known to have other serious problems [10]. Be this as it may, the general idea of a cosmological phase transition producing seeds for matter accretion in the form of global topological defects remains viable and exciting.

In this paper, we will present the first steps toward an analytical description of the spatial distribution of domain walls in generic cosmological phase transitions of a scalar field. Assuming that the scalar field has two degenerate vacuum states (+) and (−), and that, at any spatial point, the probability of being in the (+) vacuum is p and in the (−) vacuum is $1-p$, where $0 \leq p \leq 1$, we will use the results of percolation theory [13] to predict the distribution of (+) and (−) vacua and, hence, the structure of the domain walls. It is well known that such theories possess a classical phase transition; for $p < p_c$ the (+) vacua form finite clusters only, whereas for $p > p_c$ there is percolating cluster of (+) vacua. It follows that there are two fundamentally different structures of domain walls in cosmological phase transitions, depending on the value of p. If $p > p_c$ (and less than $1 - p_c$), then both (+) and (−) vacua have percolating clusters. These pass through each other in a complex interlocking way and clearly lead to large domain walls extending across all space. In [11], the authors implicitly chose $p = \frac{1}{2}$, which satisfies $p_c < p < 1 - p_c$ in three dimensions. It is these large domain walls that lead to conflict with observation. There is, however, a second possibility. If $p < p_c$, the (+) vacua are relatively small, finite islands in a vast sea of percolating (−) vacuum. It follows that all domain walls are small and compact. This scenario is just as compelling as the first, and evades the negative results of Ref. [11]. In this paper we will examine this second scenario in detail. In any theory in which $p \neq \frac{1}{2}$, it is necessary to discuss biased phase transitions. Such transitions are notoriously difficult to achieve in theories in which the scalar field is in thermal equilibrium. In this paper we present the theory of out of equilibrium phase transitions and show that this can lead to a biased vacuum probability where p need not be $\frac{1}{2}$. It is the thesis of this paper that out of equilibrium phase transitions, analyzed using percolation theory, lead to a rich domain wall structure, far more intricate and physically interesting than those considered previously. We suggest that the mechanism discussed in this paper, perhaps in conjunction with other density perturbations, such as those

arising in inflation, may be necessary to account accurately for the observed large-scale structure.

This paper is organized as follows. In Appendix A, we give a brief discussion of percolation theory, presenting, with some explanation, all the formulas required in the text. In Appendix B, we reproduce the exact values of cluster numbers for small clusters in both two and three dimensions. These numbers are essential for checking the range of validity of several crucial formula. In Sec. II we present, in some detail, the theory of percolation in two dimensions, giving all critical exponents, normalizing relevant distribution functions, and analytically and pictorially displaying crucial concepts that are much harder to visualize and intuitively understand in three dimensions. In Sec. III, we extend these results to three dimensions, presenting all critical exponents and normalizing relevant distribution functions necessary in the physical discussion in the next section. We emphasize that the results presented in Secs. II and III are not merely a review of existing literature, but an extension of such results to the regime of physical interest in this paper, a nontrivial task. Finally, we present the theory of out of equilibrium phase transitions in Sec. IV. In order to be more concrete, we then briefly present two physical scenarios to which our formalism can be applied, the first being the formation of Abell clusters and voids and the second being a computation of the contribution to the energy density fluctuations generated during a generic predecoupling transition. We give these examples merely as an illustration of how our methods work, the details being presented elsewhere.

II. PERCOLATION THEORY IN TWO DIMENSIONS

For $d = 2$, the universal critical exponents α, β, γ, δ, and ν are found to be [12]

$$\alpha = -0.69 \ , \quad \beta = 0.13 \ , \quad \gamma = 2.43 \ , \qquad \delta = 20 \ , \quad \nu = 1.35 \ . \tag{2.1}$$

The critical point p_c is not universal, having a different value for each different lattice structure. For example, for a triangular lattice $p_c = \frac{1}{2}$, whereas for a diamond lattice $p_c = 0.428$. In this section, to be concrete, we will discuss the square lattice only. For the square lattice,

$$p_c = 0.593 \ . \tag{2.2}$$

We would like to compute the cluster numbers $n_s(p)$ for any s and all values of p. For small values of s this can be done by counting the number of animals. Although this process is easy for very small s, it rapidly becomes intractable. The results for a square lattice have been computed by this method for $1 < s < 17$ and any p in Ref. [13]. Since these results are used heavily in this paper, we reproduce them in Appendix B. The cluster numbers $n_s(p)$ can also be computed in the scaling region. Define

$$z = (p - p_c)s^{\sigma} \ . \tag{2.3}$$

Then, in the limit that $p \to p_c$, $s \to \infty$, and z finite, which defines the scaling regime, it can be shown that [12]

$$n_s = q_0 s^{-\tau} f(z) \ , \tag{2.4}$$

where $f(z)$ is a universal function given by [14]

$$f(z) = 5.9003 \exp[-1.775(z' + 1)^2 + 0.2375 z'^3] \tag{2.5}$$

and $z' = z/p_c$. Note that $f(0) = 1$. This formula is valid for the range $-2.19 \lesssim z' \lesssim 1.01$. The values of σ and τ are easily computed from (2.1) and (A11). We find that

$$\sigma = 0.39 \ , \quad \tau = 2.05 \ . \tag{2.6}$$

The constant q_0 can be approximated, with reasonable accuracy, as follows. For $p = p_c$, Eq. (A4) becomes

$$\sum_s s n_s(p_c) = p_c \ , \tag{2.7}$$

where we have used the fact that $P_\infty(p_c) = 0$. Since $f(0) = 1$, it follows from (2.4) that

$$n_s(p_c) = q_0 s^{-\tau} \ . \tag{2.8}$$

Inserting this expression into (2.7), and recalling that the Riemann zeta function ζ is defined by

$$\zeta(x) = \sum_s s^{-x} \ , \tag{2.9}$$

we find that

$$q_0 = p_c / \zeta(\tau - 1) \ . \tag{2.10}$$

Using the fact that $\zeta(1.05) = 18.518$, it follows, for the square lattice, that

$$q_0 = 0.032 \ . \tag{2.11}$$

Note that q_0, in general, depends on p_c and, hence, is not a universal quantity. Inserting (2.5) and (2.11) into (2.4) yields an expression for the cluster numbers in the scaling regime given by

$$n_s = 0.1888 s^{-\tau} \exp[-1.775(z' + 1)^2 + 0.2375 z'^3] \ , \tag{2.12}$$

where, to repeat, $-2.19 \lesssim z' \lesssim 1.01$. Unfortunately, the scaling regime is not the most interesting region from the point of view of the physics discussed in this paper. It is of considerably more interest to know the cluster numbers for arbitrary p and $s \gtrsim 17$; that is, to extend our knowledge of n_s to values of s just above the animal regime. With this in mind, we rewrite (2.12) as

$$n_s = 0.1888 s^{-\tau} \exp\left\{ -1.775 \left[\left(\frac{p - p_c}{p_c} \right) s^{\sigma} + 1 \right]^2 + 2.375 \left[\left(\frac{p - p_c}{p_c} \right) s^{\sigma} \right]^3 \right\} \tag{2.13}$$

and ask how accurate this formula is away from the scaling regime. We conjecture that it remains a reasonable approximation to n_s as long as $-2.19 \lesssim [(p-p_c)/p_c]s^\sigma \lesssim 1.01$. To test this, we compute n_s using (2.13) for various values of p and $1 \leq s \leq 17$ and compare the results to the exact animal calculation. The results are plotted in Fig. 1. We see that, for $0.26 \lesssim p \lesssim 0.70$, Eq. (2.13) gives a good approximation to n_s. Below 0.26 and above 0.70 the approximation rapidly deteriorates. Note that the largest negative value of $[(p-p_c)/p_c]s^\sigma$, -1.69, is obtained for $p = 0.26$ and $s = 17$. Similarly, the largest positive value, 0.544, is obtained for $p = 0.70$ and $s = 17$. We conclude that (2.13) gives a good approximation for n_s as long as p and s are restricted so that $-1.69 \lesssim [(p-p_c)/p_c]s^\sigma \lesssim 0.544$. Thus our conjecture is almost correct, but one must consider a somewhat smaller regime for $[(p-p_c)/p_c]s^\sigma$. These results allow us to extend the calculation for n_s for s far beyond the animal regime. For example, consider $p = 0.50$. From the above discussion we know that n_s given by (2.13) is a good approximation from s equal to unity up to $s_{\max}$ satisfying $[(p-p_c)/p_c]s_{\max}^\sigma = -1.69$; that is, $s_{\max} = 444$.

We would like to compute the average cluster radius $R_s(p)$ for any s and all values of p. For small values of s, this can be done directly from the definition (A15) by computing g_{st} and $\tilde{R}_s$. Unfortunately, we can find no catalogue of such results in the literature. As we will see shortly, it is useful to compute at least one cluster radius by this method. Consider $s = 4$. The five types of $s = 4$ animals, and their animal numbers g_{4t}, are shown in Fig. 2. Note that Fig. 2(a) is the most spread out or "fractalized" of the configurations whereas Fig. 2(e) is the most compact or "droplike." Figures 2(b)–2(d) interpolate between the two. One can easily compute the radius of gyration $\tilde{R}_4$ for each of these figures using (A14). We find that $\tilde{R}_4 = 1.1180, 0.9354, 0.8660, 0.8291$, and 0.7071 for Figs. 2(a), 2(b), 2(c), 2(d), and 2(e), respectively. Note that $\tilde{R}_4$ decreases as the configurations go from more fractalized to more droplike. Inserting the values of g_{4t} and $\tilde{R}_4$ into (A15) yields the result

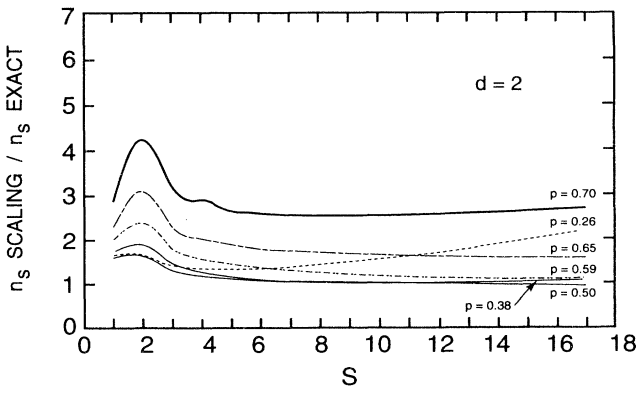

FIG. 1. This graph contains plots of the cluster number evaluated using the extension of the scaling formula divided by the exact value of the cluster number, against the cluster size s. The percolation probability takes values in the range $0.26 \leq p \leq 0.70$. The results are for a $d = 3$ square lattice.

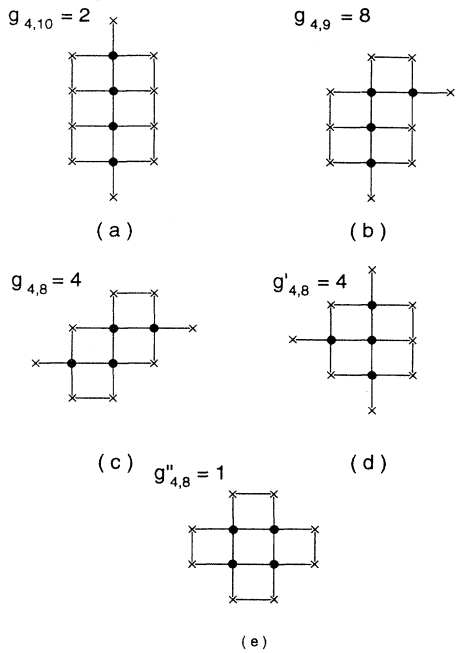

FIG. 2. (a)–(e) represent the five types of $s = 4$ animals on a square lattice for $d = 2$. The boundary of each animal and the number of each configuration are also shown.

$$R_4 = \left(\frac{7.8740 - 5.9994p + 1.2499p^2}{9.5 - 6p + p^2}\right)^{1/2} . \tag{2.14}$$

Note that, for $p = 0$, $R_4 = 0.9103$, so that the average four-cluster is more fractalized. However, for $p = 1$, $R_4 = 0.8332$, so that the average four-cluster is more droplike. The cluster radius $R_s(p)$ can also be computed in the scaling region. In the limit that $p \to p_c$, $s \to \infty$, and z finite, which defines the scaling regime, it can be shown that [12]

$$R_s = c_0 s^{\sigma\nu} R(z) , \tag{2.15}$$

where $R(z)$ is a universal function given by

$$R(z) = |z|^{\beta\delta\varphi - \nu} . \tag{2.16}$$

This formula is valid for $z = 0$ and "large" values of $|z| \neq 0$. It follows from (A20), (A21), and Refs. [15,16] that, for $z = 0$,

$$\varphi(p = p_c) = 0.5192 \tag{2.17}$$

and, for large $|z| \neq 0$,

$$\begin{aligned} \varphi(p > p_c) &= \tfrac{1}{2} , \\ \varphi(p < p_c) &= \tfrac{2}{3} . \end{aligned} \tag{2.18}$$

Note that $R(0) = 1$. Using (2.3), (2.15) can be written as

$$R_s = c_0 |p - p_c|^{\beta\delta\varphi - \nu} s^\varphi . \tag{2.19}$$

Let us consider the case when $p = p_c$. Then (2.19) becomes

$$R_s = c_0 s^{0.519} . \tag{2.20}$$

By construction, this equation is only valid for large values of s. Note, however, that z vanishes for any value s (in contrast, for $p \neq p_c$ z is no longer large for small s). One might expect, therefore, that (2.20) remains valid for small s. This turns out to be almost, but not quite, true. The correct result is

$$R_s = c_0 s^{0.519} + d_0 , \tag{2.21}$$

where d_0 is a constant that is negligibly small for large s. The constants c_0 and d_0 can be determined from a Monte Carlo calculation of R_s as a function of s^{φ} at $p = p_c$ given in Fig. 6 of Ref. [16]. We find that

$$c_0 = 0.536 , \quad d_0 = -0.214 . \tag{2.22}$$

Putting everything together, we conclude that for $p = p_c$ and any value of s (that is, $z = 0$),

$$R_s = 0.536 s^{0.519} - 0.214 . \tag{2.23}$$

For $p > p_c$ and large s (so that $|z|$ is large),

$$R_s = 0.536 |p - p_c|^{-0.050} s^{1/2} \tag{2.24}$$

and, for $p < p_c$ and large s (large $|z|$),

$$R_s = 0.536 |p - p_c|^{0.383} s^{2/3} . \tag{2.25}$$

What does one mean by large s? To answer, let us evaluate, in two dimensions, the percolation correlation length given in (A26) and (A27). The result is

$$\zeta = 0.536 (0.254)^{\varphi} |p - 0.593|^{-1.35} . \tag{2.26}$$

As discussed in Appendix A, $\zeta = R_{s_\zeta}$ where s_ζ is given by

$$s_\zeta = \left(\frac{0.593}{|p - 0.593|} \right)^{2.56} . \tag{2.27}$$

For $p = p_c (z = 0)$, $\zeta \to \infty$ and $s_\zeta \to \infty$. In this case all $s < s_\zeta$. For $p \neq p_c$, ζ and s_ζ are finite. By large s above we mean $s \gg s_\zeta$. It is important to note that, for $p \neq p_c$ but $s \ll s_\zeta$, ζ is very large with respect to R_s and this situation approaches the $p = p_c$ case. That is, for $p \neq p_c$ but $s \ll s_\zeta$, R_s is approximately given by (2.23). It is of interest to compare (2.23), (2.24), and (2.25) against the exact result for R_4 given in (2.14). For $p = p_c$, (2.14) gives $R_4 = 0.869$ whereas (2.23) predicts $R_4 = 0.886$, in good agreement. For $p = 1$, (2.14) gives $R_4 = 0.833$ whereas (2.24) yields $R_4 = 1.100$. Computing s_ζ for $p = 1$ using (2.27) we find that $s_\zeta = 2.56$. Since $s = 4$ is not much larger than $s_\zeta = 2.56$, we do not expect (2.24) to be a good approximation to R_4. In fact, the agreement is remarkably good under these circumstances and should improve readily for $s > 4$. Similarly, for $p = 0$ (2.14) gives $R_4 = 0.910$ whereas (2.25) yields $R_4 = 1.104$. Using (2.27) we find that $s_\zeta = 1$ in this case. Again, $s = 4$ is not much larger than $s_\zeta = 1$, so we do not expect (2.25) to be a good approximation to R_4. Again, the agreement is remarkably good under the circumstances and should improve for $s > 4$. We conclude that (2.23), (2.24), and (2.25) give a good approximation to R_s for $s \gtrsim 4$.

Equations (2.23), (2.24), and (2.25) can be inverted to find s as a function of p and R_s. The results are given (assuming s is large enough to ignore d_0 in the $p = p_c$ case) by

$$s = A R_s^D , \tag{2.28}$$

where for (1) $p = p_c$, any s or $p \neq p_c$, $s \ll s_\zeta$,

$$D = 1.926 , \qquad A = 3.325 , \tag{2.29}$$

(2) $p > p_c$, $s \ll s_\zeta$,

$$D = 2 , \qquad A = 3.480 |p - p_c|^{0.100} , \tag{2.30}$$

and (3) $p < p_c$, $s \gg s_\zeta$,

$$D = \tfrac{3}{2} , \qquad A = 2.548 |p - p_c|^{-0.574} . \tag{2.31}$$

As discussed in Appendix A, D is the fractal dimension of the s cluster. Note that the fractal dimension changes with p. In particular, the s cluster is more fractalized for $p < p_c$, less so for $p = p_c$, and droplike for $p > p_c$, confirming and generalizing the previous discussion for the $s = 4$ case.

Until now our discussion has been rather abstract. It is very helpful, both for understanding the above concepts and for developing physical insight into percolating systems to consider some computer generated examples. Specifically, we study several computer plots of occupied and empty sites on a two-dimensional square lattice given in Ref. [17]. We reproduce these plots, in somewhat modified form, since they give visual intuition into the structure of percolation clusters. In Fig. 3 we give the computer plot for the $p = 0.3$ case. The black dots are the occupied sites, whereas the empty sites are left white. The lattice has a total of $\eta = 49 \times 57 = 2793$ sites. It follows from the discussion in Appendix A that the number of occupied sites should be $p\eta = 838$. Counting the black dots in Fig. 3, we find a total of 880 occupied sites, in good agreement. Since $p = 0.3$ is less than $p_c = 0.593$, all occupied sites should lie in finite, nonpercolating clusters. A glance at Fig. 3 verifies that this is so. Fix s. It follows from the discussion in Appendix A that the number of s clusters should be $N_s = n_s(p = 0.3)\eta$. The cluster numbers $n_s(p)$ for $1 \leq s \leq 17$ and $p = 0.3$ are given in Appendix B and, hence, N_s can be computed in this regime. One can also count the number of s clusters of a fixed type in Fig. 3. Denote this "experimental" result by N_s^e. The theoretical and experimental results

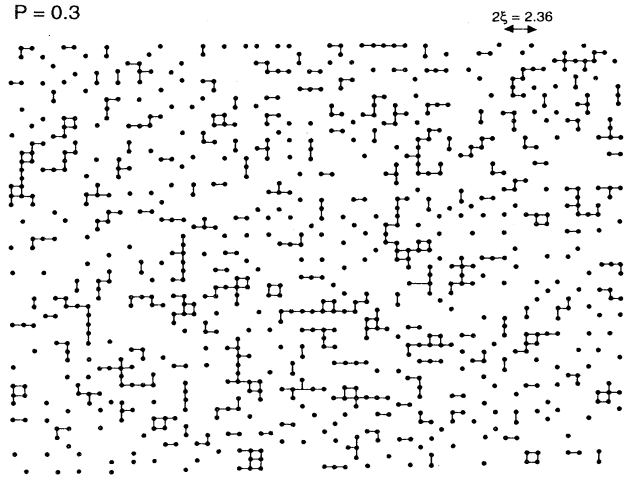

FIG. 3. Percolation theory on a $d = 2$ square lattice with $49 \times 57 = 2793$ sites. The black dots are occupied sites whereas the empty sites are white. The occupied sites have percolation probability $p = 0.3$. The percolation length ζ is displayed. Nearest neighbor occupied sites have been joined by a line, thus graphically displaying the finite s clusters.

are compared in Table I. One finds remarkable agreement. The only unexpected result is a single 18 cluster found in Fig. 2 which would be rather improbable from the point of view of percolation theory. This can be understood as follows. Using Table I, one can show that $\sum_{s=1}^{17} sN_s = 815$. But the total number of occupied sites should be 838. Hence one expects a small number of random statistical fluctuations to occur to make up the difference. The 18 cluster is such a fluctuation.

Using (2.27), one can compute s_ζ for $p = 0.3$. The result is $s_\zeta = 6$. The associated correlation length is found from (2.26) to be $\zeta = 1.18$. For $s \ll 6$, the radius of an s cluster is well approximated by (2.23). One does not expect this to work well for $s = 4$ but let us try anyway. It follows from (2.23) that $R_4 = 0.8866$. The exact value of R_4 can be computed from (2.14) for $p = 0.3$. We find that $R_4 = 0.8911$. Therefore (2.23) gives a good approximation for R_s even for $s = 4$. It follows from (2.23) that, for $s \ll 6$,

$$s = 3.325(R_s + 0.214)^{1.9267} = 3.325R_s^{1.9267} + \cdots . \tag{2.32}$$

This is similar to (2.28) and (2.29) but $s \ll 6$ are not large enough to drop the $d_0 = 0.214$ term. It follows from this expression that the fractal dimension of s clusters with $s \ll 6$ is $D = 1.9267$. To get an intuitive feeling for what this means consider, once again, the five types of $s = 4$ animals and their animal numbers g_{4t} shown in Fig. 2. It follows from the discussion preceding (A7) that the total number of each $s = 4$ animal type should be $N_{4t} = g_{4t}p^4q^t\eta$. For example, for the animal (a) in Fig. 2, $N_{4,10} = 2p^4t^{10}\eta$. For $p = 0.3$ this becomes $N_{4,10} = 1.27$. Looking on Fig. 3 for $s = 4$ clusters of type (a), we find two of them, in reasonable agreement with the percolation theory prediction. The numbers N_{4t} for all $s = 4$ animal types, and the "experimental" numbers found in Fig. 3, are presented for $p = 0.3$ in Table II. They are in reasonable agreement with one another. Now the theory predicts about one highly fractalized type (a) animal, about 17 moderately fractalized type (b), (c), and (d) animals, and about one droplike type (e) animal. If all the animals were of type (e) then one would have $D = 3$. However, the animals are spread over various animal types and correspond to more fractalization and, hence, a lower fractal dimension of $D = 1.9267$.

It is clear from Fig. 3 that the majority of the lattice sites are empty. Percolation theory predicts that the number of empty sites is $q\eta = 1955$ with $q = 1 - p = 0.7$, whereas the actual number of empty sites in Fig. 2 is 1913, in reasonable agreement. Since $q > p_c$ we expect there to be a percolating cluster of empty sites. The probability per lattice site that an empty site is part of the percolating cluster is given by P_∞ defined in Appendix A. It follows from (A4) that

$$P_\infty = 1 - \frac{\sum_s s n_s(q)}{q} , \tag{2.33}$$

where $q = 0.7$. It is easiest, and most accurate, to compute (2.33) directly, using the values of $n_s(q)$ obtained from Appendix B. These are only available for $1 \le s \le 17$ but the contributions to (2.33) of $s > 17$ are less than 1% of the total for $q = 0.7$. The result is that $P_\infty = 0.983$. Therefore percolation theory predicts that of the $q\eta = 1955$ empty sites $P_\infty q\eta = 1922$ are in the percolating cluster. Of the 1913 actual empty sites in Fig. 3, 1872 are found to be in the percolating cluster,

TABLE I. Comparison of the percolation theory prediction for the number of s clusters, N_s, against the "experimental" number of s clusters, N_s^e, found on the $p = 0.3$, 2793 site, $d = 2$ square lattice shown in Fig. 3.

s	N_s	N_s^e	s	N_s	N_s^e
1	210	220	10	2	2
2	59	69	11	2	1
3	34	33	12	1	1
4	20	23	13	(0.89)	0
5	13	17	14	(0.68)	2
6	9	5	15	(0.51)	1
7	6	4	16	(0.39)	0
8	4	6	17	(0.29)	0
9	3	4	18	(< 0.29)	0

TABLE II. Comparison of the percolation theory prediction for the number of different animal types of $s = 4$ clusters versus the "experimental" number of such clusters found on the $p = 0.3$, 2793 site, $d = 2$ square lattice shown in Fig. 3. The different $s = 4$ animal types (a)–(e) are defined in Fig. 2.

$p = 0.3$	(a)	(b)	(c)	(d)	(e)
N_{4t}	1.27	7.3	5.2	5.2	1.3
N_{4t}^e	2	8	3	8	2

again in reasonable agreement with the theory. Therefore, for $q = 0.7$, about 98% of all empty sites belong to the percolating cluster. Summarizing, the generic percolation structure of Fig. 3 is of finite occupied site s clusters, whose numerical distribution is well described by n_s, at $p = 0.3$, embedded in a percolating sea of empty sites, well described by P_∞ at $q = 0.7$.

In Fig. 4, we give the computer plot for the $p = 0.5$ case. Again, the black dots are the occupied sites whereas the empty sites are left white. This lattice also has $\eta = 49 \times 57 = 2793$ sites. The number of occupied sites should be $p\eta = 1397$. Counting the black dots in Fig. 4, we find a total of 1529 occupied sites, too large but still within 10% of the predicted value. Since $p = 0.5$ is less than $p_c = 0.593$, all occupied sites should be finite, nonpercolating clusters. A glance at Fig. 4 verifies that this is so. Fix s. It follows from the discussion in Appendix A that the number of s clusters should be $N_s = n_s(p = 0.5)\eta$. The cluster numbers $n_s(p)$ for $1 \leq s \leq 17$ and $p = 0.5$ are given in Appendix B and hence N_s can be computed in this regime. One can also count the number of s clusters of a fixed type in Fig. 4. Denote this "experimental" result by N_s^e. It is important to note that there are two distinct types of clusters in Fig. 4. The first type consists of relatively small clusters, the largest being $s = 47$. The second type clusters are much larger, the smallest having $s = 76$ (but this touches the boundary and may be a subset of a bigger cluster outside this lattice) and the largest being an internal cluster with $s = 252$. The three large internal clusters have been circled for emphasis in Fig. 4. The theoretical and experimental results for $1 \leq s \leq 17$ are compared in Table III. Again, we find remarkable agreement. The theoretical values of n_s are unknown for $s > 17$ but $N_s < 1$ in this

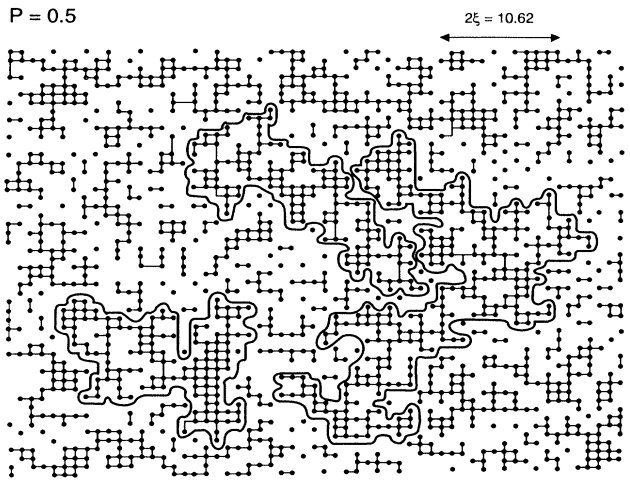

FIG. 4. Percolation theory on $d = 2$ square lattice with $49 \times 57 = 2793$ sites. The black dots are occupied sites whereas the empty sites are white. The occupied sites have percolation probability $p = 0.5$. The percolation length ζ is displayed. Nearest neighbor occupied sites have been joined by a line, thus graphically displaying the finite s clusters. The three internal large, primordial percolating clusters have each been encircled by a line for emphasis.

TABLE III. Comparison of the percolation theory prediction for the number of s clusters, N_s, against the "experimental" number of s clusters, N_s^e, found on the $p = 0.5$, 2793 site, $d = 2$ square lattice shown in Fig. 4.

s	N_s	N_s^e	s	N_s	N_s^e
1	87	89	10	2	1
2	22	35	11	2	3
3	14	7	12	2	2
4	9	5	13	2	0
5	7	5	14	1	1
6	5	3	15	1	0
7	4	5	16	1	1
8	3	3	17	(0.98)	1
9	3	3	18	(< 0.98)	1

range. One might expect, therefore, that there would be no s clusters for $s > 17$. However, using Table III, one can show that $\sum_{s=1}^{17} sN_s = 466$. But the total number of occupied sites should be 1397. Hence one expects a number of random statistical fluctuations to occur to make up the differences. Summing up the remaining small clusters gives $\sum_{s=18}^{47} sN_s = 319$. This raises the total number of occupied sites to 786, still far short of 1397. What is going on? To answer this, let us compute s_ζ at $p = 0.5$ using (2.27). The result is $s_\zeta = 118$. The associated correlation length is found from (2.26) to be $\zeta = 5.31$. Note that $2\zeta = 10.62$, the diameter of an s_ζ cluster, is on the order of 20% of the size of one side of the lattice length. That is, the correlation length is beginning to be of an appreciable size relative to the lattice. The situation is actually even more acute, since highly fractalized clusters of order $s_\zeta = 118$ can span almost the entire lattice. As discussed at the end of Appendix A, such large clusters with s of $O(s_\zeta)$ are not described by the cluster numbers n_s. Instead, they are "primordial" percolating clusters which coalesce, when ζ becomes equal to the lattice length L, into the incipient percolating cluster. The occupied sites in these large, finite, primordial clusters make up the difference between 786 and 1397. In fact, one would expect approximately $(1397 - 786)/118 = 5.17$ such clusters and, in Fig. 4, one finds 6, in good agreement.

Now note that $q = 0.5$. Since $q < p_c$ the empty sites do not percolate as they did in the $q = 0.7$ case. Instead, the empty sites behave as did the $p = 0.5$ occupied sites and need not be further analyzed. Summarizing, the generic percolation structure of Fig. 4 is of two types of finite, occupied site s clusters. The first are small clusters with $s \ll s_\zeta$ that are well described by n_s at $p = 0.5$. The second are a few large finite clusters with $s \simeq s_\zeta$, which represent primordial percolation on a finite lattice. The empty clusters have the same behavior since $q = p = 0.5$.

To conclude this section, let us recall that the physics we wish to explore in this paper, certain aspects of large-scale cosmological structure, occurs in three spatial dimensions, not in $d = 2$. So why did we analyze the $d = 2$ case in such detail? The reason is that the relevant aspects of percolation theory, finite clusters, and primordial percolating clusters, behave quantitatively the same way in three dimensions as for $d = 2$. The pictorial intuition

developed in this section, finite clusters in a vast sea of percolating vacuum and, as p approaches p_c, the growth of a few primordial percolating clusters, helps immeasurably to understand the formation of Abell clusters and large voids, great attractors, and so on in $d = 3$ percolation theory, to which we now turn.

III. PERCOLATION THEORY IN THREE DIMENSIONS

For $d = 3$, the universal critical exponents α, β, γ, δ, and ν are found to be [12]

$$\alpha = -0.43 \ , \quad \beta = 0.35 \ , \quad \gamma = 1.73 \ , \qquad \delta = 5.88 \ , \quad \nu = 0.81 \ . \tag{3.1}$$

The critical point p_c is not universal, having a different value for each different lattice structure. For example, for a body centered cubic lattice $p_c = 0.245$, whereas for a face centered cubic lattice $p_c = 0.198$. In this section, to be concrete, we discuss the simple cubic lattice only. For the simple cubic lattice,

$$p_c = 0.311 \ . \tag{3.2}$$

We would like to compute the cluster numbers $n_s(p)$ for any s and all values of p. For small values of s this can be done by counting the number of animals. Although this process is easy for very small s, it rapidly becomes intractable. The results for the simple cubic lattice have been computed by this method for $1 \leq s \leq 11$ and any p in Ref. [13]. Since these results are used heavily in this paper, we reproduce them in Appendix B. The cluster numbers $n_s(p)$ can also be computed in the scaling regime. Define

$$z = (p - p_c)s^{\sigma} \ . \tag{3.3}$$

Then, in the limit that $p \to p_c$, $s \to \infty$, and z finite, which defines the scaling regime, it can be shown that [13]

$$n_s = q_0 s^{-\tau} f(z) \ , \tag{3.4}$$

where $f(z)$ is a universal function given by [14]

$$f(z) = \exp[-0.6299z'(z' + 1.6679)] \ , \tag{3.5}$$

where $z' = z/p_c$. Note that $f(0) = 1$. This formula is valid for the range $-8.04 \lesssim z' \lesssim 5.79$. The values of σ and τ are easily computed from (3.1) and (A11). We find that

$$\sigma = 0.48 \ , \quad \tau = 2.17 \ . \tag{3.6}$$

The constant q_0 can be approximated, with reasonable accuracy, using the formula derived in Sec. II:

$$q_0 = p_c/\zeta(\tau - 1) \ , \tag{3.7}$$

where ζ is the Reimann zeta function. Using the fact that $\zeta(1.17) = 5.88$, it follows, for the simple cubic lattice, that

$$q_0 = 0.0529 \ . \tag{3.8}$$

Note that q_0 in general depends on p_c and hence is not a universal quantity. Inserting (3.5) and (3.8) into (3.4) yields an expression for the cluster numbers in the scaling regime given by

$$n_s = 0.0501 s^{-\tau} \exp[-0.6299z'(z' + 1.6679)] \ , \tag{3.9}$$

where, to repeat, $-8.04 \lesssim z' \lesssim 5.79$. Unfortunately, the scaling regime is not the most interesting region from the point of view of the physics discussed in this paper. It is of more interest to know the cluster numbers for arbitrary p and $s \gtrsim 11$; that is, to extend our knowledge of n_s to values of s just above the animal regime. With this in mind, we rewrite (3.9) as

$$n_s = 0.0501 s^{-\tau} \exp\left\{ -0.6299 \left(\frac{p - p_c}{p_c} \right) \times s^{\sigma} \left[\left(\frac{p - p_c}{p_c} \right) s^{\sigma} + 1.6679 \right] \right\} \tag{3.10}$$

and ask how accurate this formula is away from the scaling regime. We conjecture that it remains a reasonable approximation to n_s as long as $-8.04 \lesssim [(p-p_c)/p_c]s^{\sigma} \lesssim 5.79$. To test this, we compute n_s using (3.10) for various values of p and $1 \leq s \leq 11$ and compare the results to the exact animal calculation. We find that for $0.15 \lesssim p \lesssim 0.45$, Eq. (3.10) gives a good approximation to n_s. Below 0.15 and above 0.45 the approximation rapidly deteriorates. Note that the largest negative value of $[(p - p_c)/p_c]s^{\sigma}$, -1.63, is obtained for $p = 0.15$ and $s = 11$. Similarly, the largest positive value, 1.41, is obtained for $p = 0.45$ and $s = 11$. We conclude that (3.10) gives a good approximation for n_s as long as p and s are restricted so that $-1.63 \lesssim [(p - p_c)/p_c]s^{\sigma} \lesssim 1.41$. Thus our conjecture is almost correct, but one must consider a somewhat smaller regime for $[(p - p_c)/p_c]s^{\sigma}$. These results allow us to extend the calculation of n_s for s far beyond the animal regime. For example, consider $p = 0.25$. From the above discussion we know that n_s given by (3.10) is a good approximation from s equal to unity up to $s_{\max}$ satisfying $[(p - p_c)/p_c]s_{\max}^{\sigma} = -1.63$; that is, $s_{\max} = 83$.

We would like to compute the average cluster radius $R_s(p)$ for any s and all values of p. For small values of s, this can be done directly from the definition (A15) by computing g_{st} and $\tilde{R}_s$. Unfortunately, we can find no catalogue of such results in the literature. Unlike the $d = 2$ case discussed in Sec. II, the $d = 3$ animals are too complicated, even for small s, for an example to be very illuminating. The cluster radius $R_s(p)$ can also be computed in the scaling region. In the limit $p \to p_c$, $s \to \infty$, and z finite, which defines the scaling regime, it can be shown that [12]

$$R_s = c_0 s^{\sigma\nu} R(z) \ , \tag{3.11}$$

where $R(z)$ is a universal function given by

$$R(z) = |z|^{\beta\delta\rho-\nu} . \tag{3.12}$$

This formula is valid for $z = 0$ and "large" values of $|z| \neq 0$. It follows from (A20), (A21), and Refs. [15,16] that, for $z = 0$,

$$\varphi(p = p_c) = 0.3935 \tag{3.13}$$

and, for large $|z| \neq 0$,

$$\varphi(p > p_c) = \tfrac{1}{3} ,$$
$$\varphi(p < p_c) = 0.55 . \tag{3.14}$$

Note that $R(0) = 1$. Using (3.3), (3.11) can be written as

$$R_s = c_0|p - p_c|^{\beta\delta\varphi-\nu}s^{\varphi} . \tag{3.15}$$

Let us consider the case when $p = p_c$. Then (3.15) becomes

$$R_s = c_0 s^{0.393} . \tag{3.16}$$

By construction, this equation is only valid for large values of s. Note, however, that z vanishes for any value of s (in contrast, for $p \neq p_c$, z is no longer large for small s). One might expect, therefore, that (3.16) remains valid for small s. This turns out to be almost, but not quite, true. The correct result is

$$R_s = c_0 s^{0.393} + d_0 , \tag{3.17}$$

where d_0 is a constant that is negligibly small for large s. The constants c_0 and d_0 can be determined from a Monte Carlo calculation of R_s as a function of s^{φ} at $p = p_c$ given in Fig. 6 of Ref. [16]. We find that

$$c_0 = 0.702 , \quad d_0 = -0.351 . \tag{3.18}$$

Putting everything together, we conclude that, for $p = p_c$ and any value of s (that is, $z = 0$),

$$R_s = 0.702 s^{0.393} - 0.351 . \tag{3.19}$$

For $p > p_c$ and large s (so that $|z|$ is large),

$$R_s = 0.702|p - p_c|^{-0.124}s^{1/3} \tag{3.20}$$

and for $p < p_c$ and large s (large $|z|$),

$$R_s = 0.702|p - p_c|^{0.322}s^{0.55} . \tag{3.21}$$

What does one mean by large s? To answer, let us evaluate, in three dimensions, the percolation correlation length given in (A26) and (A27). The result is

$$\zeta = 0.702(0.090)^{\varphi}|p - 0.311|^{-0.81} . \tag{3.22}$$

As discussed in Appendix A, $\zeta = R_{s_\zeta}$ where s_ζ is given by

$$s_\zeta = \left(\frac{0.311}{|p - 0.311|}\right)^{2.08} . \tag{3.23}$$

For $p = p_c(z = 0)$, $\zeta \to \infty$ and $s_\zeta \to \infty$. In this case all $s < s_\zeta$. For $p \neq p_c$, ζ and s_ζ are finite. By large s we mean $s \gg s_\zeta$. It is important to note that, for $p \neq p_c$ but $s \ll s_\zeta$, ζ is very large with respect to R_s and this situation approaches the $p = p_c$ case. That is, for $p \neq p_c$ but $s \ll s_\zeta$, R_s is approximately given by (3.19). It is of interest to compare (3.19), (3.20), and (3.21) against any Monte Carlo results that may exist for R_s in three dimensions. First consider the $p = p_c$ result in (3.19). We have chosen c_0 and d_0 so that (3.19) reproduces the $p = p_c$ Monte Carlo result for R_s in Ref. [16]. This can be checked against yet another Monte Carlo result for R_s, for various values of p including p_c, in Fig. 1(b) of Ref. [16]. We reproduce these results, and compare them to (3.19), (3.20), and (3.21), in Fig. 5. Note that (3.19) closely follows the $p = p_c$ Monte Carlo results in this graph. This is an independent test of the validity of (3.19) for all values of s. What about the case where $p > p_c$? Expression (3.20) should be valid for any $s \gg s_\zeta$. Let us check this using the $p = 0.75$ case given in Fig. 5. for $p = 0.75$, it follows from (3.22) and (3.23) that $\zeta = 0.613$ and $s_\zeta = 0.49$. Hence we expect (3.20) to be a good approximation to R_s at $p = 0.75$ for all $s \gg 1$. Comparing (3.20) to the $p = 0.75$ Monte Carlo results in this graph indicates that for $s \gtrsim 10$ this is so, within a factor of 1.35. What about the $p < p_c$ case? Expression (3.21) should be valid for any $s \gg s_\zeta$. Let us check this using the $p = 0.1$ case given in Fig. 5. For $p = 0.1$, it follows from (3.22) and (3.23) that $\zeta = 0.658$ and $s_\zeta = 2.24$. Hence we expect (3.21) to be a good approximation to R_s at $p = 0.1$ for all $s \gg 2$. Comparing (3.21) to the $p = 0.1$ Monte Carlo results in this graph indicates that for $s \gtrsim 10$ the agreement is almost exact. We conclude that (3.19), (3.20), and (3.21) give a good approximation to R_s in their expected regime of validity.

Equations (3.19), (3.20), and (3.21) can be inverted to find s as a function of p and R_s. The results are given

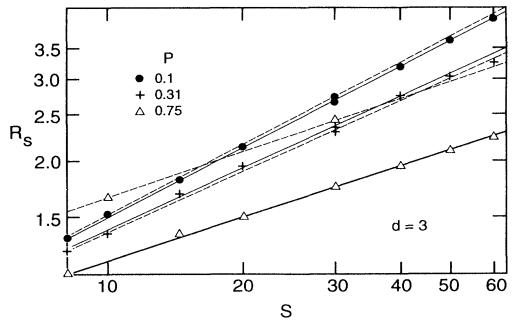

FIG. 5. Each line is a plot of cluster radius R_s against the cluster number s on a $d = 3$ simple cubic lattice. The solid lines are the results of Monte Carlo percolation "experiments" for three different values of percolation probability p. The dashed lines are extensions of the scaling formulas for the cluster radius to small values of s for the same three values of p.

(assuming s is large enough to ignore d_0 in the $p = p_c$ case) by

$$s = AR_s^D \ , \tag{3.24}$$

where for (1) $p = p_c$, any s or $p \neq p_c$, $s \ll s_\zeta$,

$$D = 2.544 \ , \qquad A = 2.460 \ , \tag{3.25}$$

(2) $p > p_c$, $s \gg s_\zeta$,

$$D = 3 \ , \qquad A = 2.891|p - p_c|^{0.372} \ , \tag{3.26}$$

and (3) $p < p_c$, $s \gg s_\zeta$,

$$D = 1.818 \ , \qquad A = 1.903|p - p_c|^{-0.585} \ . \tag{3.27}$$

As discussed in Appendix A, D is the fractal dimension of the s cluster. Note that the fractal dimension changes with p. In particular, the s cluster is more fractalized for $p < p_c$, less so for $p = p_c$, and droplike for $p > p_c$.

It follows from (A3) or (A4) that the percolation probability P_∞ is given by

$$P_\infty = 1 - \sum_s \frac{sn_s}{p} \tag{3.28}$$

for $p > p_c$, and vanishes for $p \leq p_c$. In the next section, where we discuss the role of percolation theory in large-scale structures, we will always take the occupied sites to have $p < p_c$. Therefore, for the occupied sites, $P_\infty = 0$, there is no percolating cluster and all such s clusters are finite. In this case, however, the empty states satisfy $q > 1 - p_c = 0.689$. Since $q > p_c$, P_∞ is nonvanishing for the empty sites and there is a percolating empty cluster. Furthermore, since q is considerably bigger than p_c, we expect the percolating cluster to be very large and P_∞ to be near unity. This can be explicitly checked using the animal results in Ref. [13] and reproduced in Appendix B. Unfortunately, these results are for $q \leq 0.5$. Let us calculate P_∞ for $q = 0.5$, knowing that P_∞ is larger for $q > 0.5$. Using Appendix B and (3.28) we find that, for $q = 0.5$, $P_\infty = 0.96$. Therefore, for $q > 0.689$, $P_\infty > 0.96$. That is, in excess of 96% of the empty sites are in the percolating cluster. We conclude that, for $d = 3$, when $p < p_c$, the occupied sites all form into relatively small finite clusters embedded in a vast sea of percolating empty sites, the finite cluster empty sites being negligible.

IV. NONEQUILIBRIUM PHASE TRANSITIONS

In this section we discuss a mechanism for phase transitions in a scalar field ϕ, all of whose couplings are so small as to render the field out of thermal equilibrium. The potential energy of this scalar is assumed to have at least two degenerate minima with vanishing cosmological constant. Furthermore, we assume that the universe goes through a period of inflation followed by a period of Friedmann-Robinson-Walker (FRW) expansion. It is supposed that inflation is due to some other mechanism, perhaps a different inflation scalar field, but is not caused by scalar ϕ. On the contrary, we assume that the height of the ϕ potential energy between the minima is very much smaller than the Hubble parameter at the time of inflation.

The dynamics of an out of equilibrium scalar field existing on an inflating de Sitter space breaks into two pieces. First, there is a classical field ϕ_c, which satisfies the classical equation of motion

$$\ddot{\phi}_c + 3H\dot{\phi}_c + \frac{dV}{d\phi_c} = 0 \ , \tag{4.1}$$

where V is the potential of ϕ and H is the Hubble parameter. We have assumed in (4.1) that the spatial gradient terms have been exponentially driven to zero by inflation. Now, during inflation, and long afterward, H is very large (by assumption) compared to the potential and its derivatives. It follows that we may drop the $dV/d\phi_c$ term in (4.1) and the resulting equation is solved by $\phi_c = c$, where c is an arbitrary constant. To next order, there is an extremely tiny damped velocity $\dot{\phi}_c \sim (dV/d\phi_c)/H$ which one may safely ignore. Therefore, during inflation, and long afterward, ϕ_c is, to extreme accuracy, an arbitrary constant. We emphasize that there is no information in the theory which could fix the value of c. It is completely arbitrary. We will make the standard assumption that our present horizon is embedded in an enormous inflation horizon, created by exponentially blowing up a single causal horizon in the distant past. It follows that $\phi_c = c$ will be the same over the entire inflationary horizon. Note that since our theory is not in thermal equilibrium, there are no thermal corrections to potential V. Hence there are no thermal effects forcing $\phi_c = 0$ or to any other value. In our case, ϕ_c is an arbitrary constant. Second, we must consider the quantum fluctuations of the quantum field $\hat{\phi}$ in the de Sitter space background. As is well known, and discussed widely in the literature [18], there are quantum fluctuations impressed on the vacuum state of ϕ due to the boundary conditions of de Sitter space. These fluctuations are sometimes referred to as contributing to the "Hawking temperature" of de Sitter space but, in fact, they are not true thermal effects. These fluctuations can be described by a "quasiclassical" scalar field ϕ_q, which contains Fourier components with wavelengths ranging from the size of the particle horizon during inflation, H_i^{-1} where H_i is the initial Hubble parameter, all the way out to the inflation horizon $H_i^{-1}e^{H_i t_e}$, where t_e is the time at the end of inflation. Now at any point x these spatial fluctuations lead to fluctuations in the value of ϕ, in field space, around $\phi_c = c$. These can be described by a Gaussian distribution centered at ϕ_c with width σ_l, given by

$$P(\phi) = \frac{1}{\sqrt{2\pi}\sigma_l} e^{-(\phi-\phi_c)^2/2\sigma_l^2} \ . \tag{4.2}$$

The value of σ_l depends on the range of spatial fluctuation wavelengths one wants to consider. In general, if we consider wavelengths from small size l_c up to larger size l, then these induce fluctuations at x with a width

$$\sigma_l^2 = \frac{H_i^2}{4\pi^2} \ln\left(\frac{l}{l_c}\right) . \tag{4.3}$$

For example, if we want to include the effect of all wavelengths in the quasiclassical field at the moment that inflation ends, then we would take $l_c = H_i^{-1}$ and $l = H_i^{-1} e^{H_i t_e}$. It is important to note that, since these fluctuations are generated in a homogeneous way on the inflating spatial manifold, the formulas for the Gaussian distribution (4.2) and width (4.3) are the same for any two points x and y within one inflation horizon.

Now after inflation ends and the FRW period begins, the Hubble parameter begins to decrease and hence the size of the particle horizon to grow. As the particle horizon grows, the smaller-wavelength Fourier components of the quasiclassical field ϕ_q begin to enter the horizon. As they do, they start to oscillate, their amplitudes become exponentially damped in time, and they can effectively be ignored. Hence, at any redshift z during the FRW expansion phase, the quasiclassical field ϕ_q is composed only of those Fourier modes with wavelengths from the size of the particle horizon at z, $H(z)^{-1}$, out to the size of the inflation horizon. As a consequence, the distribution of spatial fluctuations at any point x at redshift z is still given by (4.2), but where σ_l is to be evaluated using $l_c = H(z)^{-1}$. Note, however, that since the change in l_c relative to the inflation horizon radius during this period is not dramatic, it follows from (4.3) that the fluctuation distribution is relatively stable. It is also of interest to compute the expectation value of the Hamiltonian density, $\hat{H}$, at any point x at redshift z during the FRW phase. Generically, we find that

$$\langle \hat{H}(x) \rangle \simeq H_i^2 H(z)^2 . \tag{4.4}$$

As long as $\langle \hat{H}(x) \rangle$ is greater than the height of the potential energy V, and this has been assumed in all of the above discussion, then the fluctuations are "hot" and can freely jump back and forth from one to another. Therefore, the vacuum does not settle down into a specific value but, rather, it retains the random character described by (4.2) and (4.3).

Eventually, after a long time, H decreases to a point where the damping term in the equation of motion, $3H\dot{\phi}$, becomes comparable to the potential term $dV/d\phi$. At this time, which we designate by the redshift z_t (t for transition) the potential V can no longer be ignored and we must reanalyze both the classical and quantum contributions to the ϕ vacuum. It is not hard to show that z_t is also the redshift at which $\langle \hat{H}(x) \rangle$ becomes comparable to the height of the potential V. What changes take place at z_t and thereafter? Under the force of the $dV/d\phi$ term in the equation of motion, both ϕ_c and each fluctuation around ϕ_c begin to roll toward the nearest minimum in V. If we, henceforth, assume that the width of (4.2) at z_t is of the same order of magnitude as the distance v between two adjacent minima of V, that is,

$$\sigma_l(z_t) \simeq v , \tag{4.5}$$

then it is clear that we need only consider the two adjacent minima of V nearest to $\phi_c = c$. Let us call the minimum to the right of ϕ_c the (+) vacuum and the minimum to the left of ϕ_c the (−) vacuum. Furthermore, we will center the zero of ϕ space, $\phi = 0$, to be at the top of the potential hill between (+) and (−). It is clear then that, under the force of the $dV/d\phi$ term, any field to the right of $\phi = 0$ will roll into the (+) vacuum and any field to the left of $\phi = 0$ will roll into the (−) vacuum. Furthermore, from the distribution (C2), we know that the probability that a vacuum fluctuation will be to the right of $\phi = 0$ and hence roll to the (+) vacuum is given by

$$p = \int_0^\infty d\phi\, P(\phi) , \tag{4.6}$$

where σ_l is evaluated at redshift z_t.

Since ϕ_c is arbitrary, it follows that p can take any value in the range $0 \le p \le 1$ and need not be $\frac{1}{2}$. Clearly, the probability that a fluctuation will roll to the (−) vacuum is $1 - p$. It is also important to note that after z_t $\langle \hat{H}(x) \rangle$ becomes smaller than the height of the potential. Therefore the system becomes "cold." Once a fluctuation occurs, say to the (+) vacuum, it is impossible for it to then jump to the (−) vacuum since there is not enough energy density to get over the potential barrier between the two minima. Therefore, at any point x at z_t or shortly thereafter, the field must choose the (+) vacuum with probability p or the (−) vacuum with probability $1 - p$, where p lies in the range $0 \le p \le 1$ but is otherwise arbitrary. This type of out of equilibrium phase transition, with "biased" probability of being in one vacuum as opposed to another, was first introduced in [10]. We refer to the reader there for more details. This justifies our use of $p \neq \frac{1}{2}$ percolation theory in this paper.

To proceed it is useful to give an explicit example for the scalar field theory. We will, for simplicity, consider the simplest relevant scalar field potential. Our results, however, are essentially unchanged for any other scenario of this type. Consider a real scalar field ϕ which has, as its Lagrangian,

$$\mathcal{L} = \tfrac{1}{2} g^{\mu\nu} \partial_\mu \phi \partial_\nu \phi + \frac{m^2}{2}\phi^2 - \frac{\lambda}{4!}\phi^4 - \frac{3}{2\lambda} m^4 , \tag{4.7}$$

where $g_{\mu\nu}$ is the Robinson-Walker metric with the line element

$$ds^2 = dt^2 - R^2(t) \left\{ \frac{dr^2}{1 - kr^2} + r^2 d\theta^2 + r^2 \sin^2\theta\, d\phi^2 \right\} . \tag{4.8}$$

In general, k can take the values +1, 0, or −1. However, we will assume that Ω, the ratio of the total energy density to the critical density ρ_c, is unity. This then implies that k vanishes. We henceforth take $\Omega = 1$ and $k = 0$. The potential energy

$$V(\phi) = -\frac{m^2}{2}\phi^2 + \frac{\lambda}{4!}\phi^4 + \frac{3}{2\lambda} m^4 \tag{4.9}$$

is minimized by two separate vacua

$$\langle\phi\rangle = \pm\sqrt{\frac{6}{\lambda}}m \ , \tag{4.10}$$

both of which have vanishing cosmological constant. It is well known that there is a static kink solution interpolating between these two vacua which, in the rescaled coordinate x perpendicular to its surface, is given by

$$\phi(x;x_0) = \sqrt{\frac{6}{\lambda}}\tanh\left(\frac{m}{\sqrt{2}}(x-x_0)\right) \ , \tag{4.11}$$

where x_0, the location of the kink, is arbitrary. The width of the kink is well described by $\Delta = \sqrt{2}/m$ and the zero-zero component of its stress-energy tensor is found to be

$$T_{00} = \frac{3m^4}{\lambda}\left[1-\tanh^2\left(\frac{m}{\sqrt{2}}(x-x_0)\right)\right]^2 \ . \tag{4.12}$$

The kink solution (4.11) defines a domain wall between the regions of space with different vacuum structure. The width of this domain wall is, again, $\Delta = \sqrt{2}/m$ and the energy density at its center, the value of T_{00} at $x = x_0$, is $\rho_{\rm DW} = 3m^4/\lambda$. The surface energy density of the domain wall, defined by $\eta = \int_{-\infty}^{+\infty} T_{00}\,dx$, is found to be

$$\eta = \frac{4}{3}\frac{\langle\phi\rangle^2}{\Delta} \ . \tag{4.13}$$

The requirement that the ϕ field be out of thermal equilibrium immediately implies that $\lambda \ll 1$. Furthermore, since the height of the potential barrier must be much smaller than H_i^4 during inflation, it follows that m has to be very tiny.

We can now return to the discussion of the nonequilibrium phase transition. At the redshift z_t the scale of fluctuations, $\langle\hat{H}\rangle$, falls below the height of the potential, and also the Compton wavelength of the scalar field, $\lambda_c = 1/m$, becomes smaller than the horizon scale, $\lambda_c < H^{-1}$. As discussed above, the field must then roll to the (+) vacuum with probability p or the (−) vacuum with probability $1-p$. Whichever way it rolls, there will be a period of coherent oscillations around the vacuum until, at the redshift we will denote by z_i, the field comes approximately to rest at the minimum. It follows that between z_t and z_i the potential barrier is not clearly visible above the background energy density due to these oscillations and hence domain walls do not form. It is only after z_i, when the height of the potential becomes significantly larger than the energy of the oscillating background, that stable domain walls can occur. When one considers the equation of motion for a generic scalar field one finds that the zero-mode solution behaves as $\phi(t) = A(t)\cos(mt)$ which, after averaging over the period of oscillations, gives the average energy density of the background equal to $\rho_{\rm osc}(t) = \frac{1}{2}A^2(t)m^2$ (A denotes the amplitude of oscillations). Assuming adiabatic expansion during the matter dominated epoch one obtains the energy conservation law in the form $(d/dt)[A^2(t)m^2R^3(t)/2] = 0$. It follows that, in terms of redshifts, the oscillation energy density evolves as

$$\rho_{\rm osc}(z) \approx \frac{(1-\epsilon)^2\langle\phi\rangle^2}{\Delta^2}\left(\frac{1+z}{1+z_t}\right)^3 \ , \tag{4.14}$$

where $0 < \epsilon < 1$, $z < z_t$, and $(1-\epsilon)\langle\phi\rangle$ is a typical amplitude of ϕ at z_t. Here we discuss a transition occurring during the matter dominance. Similar reasoning applies if the transition occurs during the radiation dominated epoch. It is easy to see that these coherent oscillations behave like matter. Then we find using (4.14) and (4.13) that the ratio of the energy density of the oscillating vacuum to the height of the potential barrier is

$$\frac{\rho_{\rm osc}}{\eta/\Delta} \approx \frac{(1-\epsilon)^2(1+z)^3}{(1+z_t)^3} \ . \tag{4.15}$$

The coefficient of proportionality is easily shown to be smaller than unity. Hence, at z_t, $\rho_{\rm osc}$ is approximately the same as the potential height but quickly decreases relative to it with time. For concreteness, we will define z_i as the redshift at which $\rho_{\rm osc}/(\eta/\Delta) = 10^{-2}$. Then it is easy to see that z_i is related to z_t through the equation

$$1 + z_i = \tfrac{1}{2}(1+z_t) \ , \tag{4.16}$$

so if for example $z_i = 10^3$ then $z_i = 500$, and so on. In order to see whether the vacuum oscillations can dominate the energy density of the Universe, let us compare $\rho_{\rm osc}$ with ρ_b where ρ_b is the energy density of the baryonic component of the Universe. Denoting the present value by ρ_{bo}, and noting that $\rho_b(z) = \rho_{bo}(1+z)^3$ and taking $\epsilon \ll 1$ one obtains

$$\frac{\rho_{\rm osc}}{\rho_b}(z) \approx 10^{-83}\frac{\langle\phi\rangle^2}{\rho_{bo}} \ , \tag{4.17}$$

which is independent of z. The requirement that the ratio (4.17) is smaller than unity results in an upper bound on the $\langle\phi\rangle$ which is found to be $\langle\phi\rangle < 2\times10^{18}$ GeV, which is satisfied in all physically relevant theories. To conclude this paragraph, we stress again that it is at z_i rather than at z_t when the stable domain walls effectively form.

Let us describe this initial distribution of walls in some detail. To this end we now make two important assumptions. The first is that, at redshift z_i, if the system is in the $+\sqrt{(6/\lambda)}m$ state [henceforth called the (+) vacuum] at some point in space, then that point is necessarily contained in a three-dimensional volume, of order Λ_i^3, all of whose points are also in the (+) vacuum. The same is assumed to be true for spatial points in the $-\sqrt{(6/\lambda)}m$ state [henceforth called the (−) vacuum]. That is, three-dimensional space at redshift z_i is assumed, as far as the vacuum structure is concerned, to be partitioned into a lattice with lattice spacing Λ_i. Since domain walls of width Δ will occur between lattice sites of different vacua, Λ_i must satisfy

$$\Lambda_i = l\Delta \ , \tag{4.18}$$

where l is a small real number satisfying $l \gtrsim 2$. Second, we assume that the probability that a lattice site is in the (+) vacuum is p, where $0 \le p \le 1$, and the probability that a site is in the (−) vacuum is $q = 1-p$. We further demand that there is no correlation between the

vacuum structures of any two different lattice sites. Subject to these two assumptions, the spatial distribution of the (+) and (−) vacua at redshift z_i can be computed using three-dimensional percolation theory. The second of these assumptions is very nontrivial and requires justification. To begin with, we emphasize that the extremely small value of the coupling parameters of the ϕ field ensures that the system is completely out of thermal equilibrium. Hence one cannot apply temperature dependent field theory to analyze the ϕ phase transition. This is important because it is well known that equilibrium phase transitions lead to the unique choice of $p = \frac{1}{2}$ and are beset with additional difficulties [19]. Our theory, because it is completely out of thermal equilibrium, avoids these problems.

Let V_i be the volume of space at redshift z_i. For concreteness, we will assume that the minimal vacuum volume is a cube of volume Λ_i^3. Then, as far as the vacuum structure is concerned, space at redshift z_i is a three-dimensional cubic lattice with lattice spacing Λ_i and $N_i = V_i/\Lambda_i^3$ lattice sites. Since the main results of this section depend, primarily, on universal quantities, we are justified in choosing a specific lattice to carry out our analysis. Having chosen the cubic lattice, all the results of Sec. III can be used. In this section, we will always assume that

$$p < p_c(= 0.311) \ . \tag{4.19}$$

It follows from the discussion in Sec. III and Appendix A that all lattice sites in the (+) vacuum lie in finite, nonpercolating s clusters. The total number of sites in the (+) vacuum is given by $N_{(+)} = pN_i$. Of particular importance is the analytic expression for the cluster numbers n_s of (+) vacuum, finite s clusters. These were shown in Sec. III to be given by

$$n_s = 0.0501 s^{-\tau} \exp\left\{ -0.6299 \left(\frac{p - p_c}{p_c} \right) \right.$$
$$\left. \times s^{\sigma} \left[\left(\frac{p - p_c}{p_c} \right) s^{\sigma} + 1.6679 \right] \right\} , \tag{4.20}$$

where $\tau = 2.17$, $\sigma = 0.48$, and p and s are restricted to satisfy $-1.63 \lesssim [(p - p_c)/p_c] s^{\sigma} \lesssim 1.41$. The values of p and s relevant to our analysis will lie comfortably within this range. The total number of s clusters at redshift z_i is then given by $N_s = n_s N_i$. Since $p < p_c$, then $q > 1 - p_c(= 0.689)$. It follows from the discussion at the end of Sec. III that in excess of 96% of all sites in the (−) vacuum lie in the percolating cluster, which extends across the entire spatial volume. Hence all (−) vacuum lattice sites which lie in finite s clusters can simply be ignored. The total number of (−) vacuum sites is given by $N_{(-)} = qN_i$. Note that $N_{(-)} > N_{(+)}$. We conclude that space is dominated by a vast, percolating sea of (−) vacuum, with relatively small, finite islands of (+) vacuum embedded in it. The structure of the finite (+) vacuum clusters is very much controlled by the percolating correlation length ζ. For $p < p_c$, it follows from (3.22) that

$$\zeta = 0.187 |p - p_c|^{-0.81} \Lambda_i \ , \tag{4.21}$$

where we have made ζ dimensional by introducing the physical lattice spacing Λ_i. The associated cluster size is given by

$$s_\zeta = \left(\frac{0.311}{0.311 - p} \right)^{2.08} \ . \tag{4.22}$$

As discussed in Sec. III, the average radius of gyration R_s and the fractal dimension D of the finite (+) vacuum s clusters depend on the size of s relative to s_ζ. When $s \gg s_\zeta$, then it follows from (3.21) that

$$R_s = 0.702 |p - p_c|^{0.322} s^{0.55} \Lambda_i \ . \tag{4.23}$$

This equation can be inverted to give

$$s = 1.903 |p - p_c|^{-0.585} \left(\frac{R_s}{\Lambda_i} \right)^{1.818} \ . \tag{4.24}$$

The fractal dimension of such a cluster is $D = 1.818$. The fact that $D < 3$ implies that these s clusters are not droplike and exhibit considerable fractal behavior such as discussed, in two dimensions, in Sec. II. Now for $s \ll s_\zeta$ the structure of the finite (+) vacuum s clusters is somewhat different. It follows from the discussion in Sec. III and (3.19) that

$$R_s = (0.702 s^{0.393} - 0.351) \Lambda_i \ . \tag{4.25}$$

This equation can be inverted to give

$$s = 2.460 \left(\frac{R_s}{\Lambda_i} + 0.351 \right)^{2.544} \ . \tag{4.26}$$

The fractal dimension of such a cluster is $D = 2.544$. Again, since $D < 3$, such clusters are not droplike and exhibit mild fractal behavior. No matter what the size of s is relative to s_ζ, a finite (+) vacuum s cluster has a boundary containing t_s lattice sites of (−) vacuum where

$$t_s = \left(\frac{1 - p}{p} \right) s - (1 - p) \frac{\partial}{\partial p} \ln n_s \ , \tag{4.27}$$

as discussed in Appendix A. Using (4.20), it is a bit messy, but straightforward, to show that the second turn in (4.27) is much smaller than the first and hence t_s is well approximated by

$$t_s = \left(\frac{1 - p}{p} \right) s \ , \tag{4.28}$$

when $p < p_c$ and $s \gtrsim 10$. The values of s relevant to our discussion will always satisfy this bound. The properties of the boundary of an s cluster are more complicated than one might at first realize. To begin with, the boundary need not be totally external. Some, or many, of the boundary points can lie inside the s cluster. Furthermore, if $D = 3$ (which, for $p < p_c$, it is not) then the boundary, both external and internal, would form a smooth surface. However, in our case $D < 3$ and the

boundary becomes fractalized, more for $s \gg s_\zeta$ and less so in the $s \ll s_\zeta$ case. Let us denote by f the average number of faces of the lattice cube surrounding a boundary point that directly touch the s cluster. Of course, f must satisfy $1 \leq f \leq 6$. If $D = 3$, then $f = 1$. However, for $D < 3$ the fractal behavior of the boundary allows more surfaces to touch the s cluster. For example, an isolated $(-)$ vacuum point totally inside the s cluster would have six faces touching the cluster. We have not computed f analytically for $D < 3$. A cursory numerical study indicates that $2 < f < 4$. Fortunately, we do not need to know the exact value of f in the following analysis. Note that the average surface area of any finite $(+)$ vacuum s cluster is given by

$$A_s = t_s f \Lambda_i^2 \ . \tag{4.29}$$

As discussed previously, between any nearest neighbor $(+)$ and $(-)$ vacuum sites there will be a domain wall with surface energy density η given in (4.13). It follows that a finite $(+)$ vacuum s cluster is bounded by a domain wall with average total energy:

$$\delta M_s = \eta A_s \ . \tag{4.30}$$

In the preceding, we have focused on the vacuum structure of the biased phase transition and the properties of the associated domain walls at redshift z_i. This discussion presumed that $\Omega = 1$ and therefore that $k = 0$ in the Robinson-Walker metric (4.8). In order to make a connection to the present-day observed matter distribution we have to assume a specific scenario for the development of the wall system and that of the induced fluctuations in the energy density of the matter content of the Universe. Several scenarios are possible, two viable examples being presented in detail in [20] and [21]. In general, details of the evolution of matter-wall systems depend on the epoch when the transition takes place. If z_i happens to lie deeply in the radiation dominated epoch, then the system evolves as described in [21]. The accretion of matter onto walls is greatly slowed down with respect to the predictions of the spherical collapse model [22]. Furthermore, wall bags with radii fitting our horizon annihilate before photon decoupling or their abundance is very strongly suppressed, so that they do not distort the microwave background. As demonstrated in [21] this scenario gives rise to a significant wall-induced contribution to the total $\delta\rho/\rho$ spectrum, which is strongly suppressed at small scales, but significant at large scales. This additional spectrum can add significantly to a cold dark matter (CDM) spectrum at intermediate scales and at the same time give an observable signal at the Cosmic Background Explorer (COBE) scales, as required by current data. The other possibility, discussed in [20], is that the transition takes place after photon decoupling so the walls do not leave any direct imprint on the last scattering surface. In this case, however, one has to compute the postdecoupling distortions of the photon background due to the gravitational potential of domain wall bags. In first approximation, this is taken care of by fulfilling the limit on the wall tension η arising from the formula

$$\frac{\delta T}{T} \approx 8\pi G_N \eta H^{-1} \ , \tag{4.31}$$

where G_N denotes the Newton constant and H^{-1} is the horizon size at the time when the photon passes the wall [23]. In the case of stable walls, one puts into (4.31) the present-day horizon size instead of H^{-1}, but, since our wall bags are not stable and rapidly disappear, we have to use the formula (4.31) in its basic form. This formula, when one requires that $\delta T/T \leq 1 \times 10^{-5}$, gives an upper bound on the ratio $\eta/H(z_i)$ of

$$\frac{\eta}{H(z_i)} \leq 4 \times 10^{-7} M_P^2 \ , \tag{4.32}$$

which transfers into an upper limit on $\langle\phi\rangle$ given by

$$\langle\phi\rangle^2 \leq 3 M_P^2 \frac{H(z_i)}{m} \ . \tag{4.33}$$

Again, this limit is not difficult to satisfy and it is obeyed by all the examples presented in [20,21]. To indicate all the possibilities offered by the second approach, where it is more likely that the pattern of wall bags would directly correspond to the observed distribution of galaxies, one has to distinguish two distinctly different physical regimes within the restriction $p < p_c$. The first is for p sufficiently small that the percolation correlation length is much smaller than the observable lattice size at z_i. That is, $\zeta(z_i) \ll N_i^{1/3} \Lambda(z_i)$. In this regime, one predicts only small matter clusters well described by n_s in (4.20). The second regime occurs as p approaches p_c, and the correlation length becomes comparable to the lattice size at z_i. That is, $\zeta(z_i) \approx N_i^{1/3} \Lambda(z_i)$. In this case, in addition to smaller matter clusters described by n_s, there are few, large "primordial" percolating matter clusters. These, while not actually percolating, are much larger than the smaller clusters. These two regions are the analogue of those studied in $d = 2$. We refer the reader to Sec. II to gain physical intuition about them. The second regime might be considered as a realization of the "bubbly" Universe, where there exist large voids (corresponding to large, "almost percolating" clusters). In this model matter would accrete to the surface of these voids forming a frothy foam or bubblelike structure. This generic picture seems to be in basic agreement with observation.

We close this section by pointing out that the final, stable vacuum state of a scalar field with potential energy (4.3), when evaluated on a three-dimensional lattice, is that of the $d = 3$ Ising model. From this point of view, the percolation theory results discussed in this paper represent the initial unstable state of the theory at redshift z_i. This state will relax in time toward the stable Ising model vacuum. In this paper, we have referred to this relaxation as the dynamical motion of the domain walls, which is the same thing. The effect of dynamics in our scenario is expected to be relatively small, and will be discussed elsewhere.

V. CONCLUSIONS

We have demonstrated in this paper how percolation theory can be used to analytically compute both the qualitative and quantitative features of the initial conditions for large-scale structure formation induced by a cosmological phase transition in an out of thermal equilibrium scalar field. In closing we would like to emphasize two points. The first is that our scalar field ϕ is a new field, whose only physical role is to induce either all, or part, of observed large-scale structure. To distinguish it from all other scalar fields that may occur in cosmology, like the inflaton, or in particle physics, like the Higgs boson, we would like to give ϕ a name, the "structuron." Second, we point out that, although for postdecoupling transitions we expect the matter clustering to resemble the main features of the original wall distribution, in general there is a complicated dynamics of the matter-wall system which leads from the initial conditions at redshift z_i described in this work to the observed large-scale structure. The analysis of this dynamics lies beyond the scope of this paper, the more detailed discussion of the examples corresponding to different regimes being presented in Refs. [21,20].

ACKNOWLEDGMENTS

We would like to thank Paul Steinhardt, David Spergel, and Rick Davis for many interesting conversations. We also acknowledge useful discussions with Ram Brustein. We would especially like to thank Tom Lubensky and Brooks Harris for informative discussions on the intricacies of percolation theory. The work of B.A.O. was supported in part by the DOE under Contract No. DOE-AC02-76-ERO-3071.

APPENDIX A: PERCOLATION THEORY

This appendix is intended to acquaint the reader with the concepts and formulas of percolation theory necessary to comprehend the main body of the text. All material in this appendix can be found in [12,17] and references therein. The arena of percolation theory is a d-dimensional lattice containing N^d lattice sites. N can be finite, but the "thermodynamic" limit is obtained by letting $N \to \infty$. The structure of the lattice is not unique. For example, in three dimensions, the lattice may be simple cubic, or body centered cubic, or face centered cubic, or even random. In physical applications, there is a length associated with nearest neighbor lattice sites, generically denoted by Λ. It follows that each side of the lattice has length $L = N\Lambda$ and that the lattice volume is L^d.

Percolation theory is defined on such a lattice as follows. Assume that every individual lattice sites can be in one of two states, either "occupied" or "empty." Furthermore, assume that each site is occupied or empty entirely randomly, independent of the state of its neighbors. It follows that the entire theory, for a given lattice structure, is defined by the probability p ($0 \leq p \leq 1$) that an individual site is occupied. The probability that a site is unoccupied is clearly $q = 1-p$. To be precise, percolation theory defined in this manner is called site percolation theory. It is possible to define so-called bond percolation theory, where the links between nearest neighbor lattice sites are assumed to be either "open" or "closed" with probability p and $1-p$, respectively, independent of the state of neighboring links. Site and bond percolation theory are identical in many respects, differing only (from the point of view of this paper) in inessential aspects. Hence, in what follows, we discuss only site percolation theory.

Consider percolation theory defined on some lattice. The occupied sites are either isolated from one another or they form small groups of neighbors. These groups are called clusters. An s cluster is defined as a group of s occupied lattice sites connected by nearest neighbor distances. In a large lattice, there are more s clusters than in a small lattice and hence the total number of such clusters is not a fundamental quantity. However, the total number of s clusters divided by the number of lattice sites N^d is a fundamental quantity, and is denoted by n_s. That is, n_s is the probability per lattice site that that site is a fixed element of an s cluster. It is important to note that n_s is, in general, a function of p. By definition, the total number of s clusters, N_s, is given by

$$N_s = n_s N^d \ . \tag{A1}$$

Also, it follows from the above definition that the probability that a given lattice site is any element of an s cluster is given by

$$P_s = s n_s \ . \tag{A2}$$

An s cluster that extends from one end of the lattice to the other is called a percolating or infinite (since in the thermodynamic limit $N \to \infty$ this cluster would have $s \to \infty$) cluster. Any other s cluster is called a finite cluster. For small values of p one finds only finite clusters, whereas for large p a single percolating cluster (as well as finite clusters) is found to exist. One never finds two or more percolating clusters. It follows that at some critical probability, denoted p_c, there is a phase transition such that for $p > p_c$ a unique percolating cluster exists, whereas for $p < p_c$ all clusters are finite. Exactly at $p = p_c$ there also is a percolating cluster which, however, has the property that the fraction of sites belonging to it goes to zero as $N \to \infty$. Hence the percolating cluster at $p = p_c$ is called the "incipient" percolating cluster.

We define the percolation probability P_∞ to be the fraction of occupied sites belonging to the percolation cluster relative to the total number of lattice sites N^d. Note that P_∞ is a function of p. It follows from the above that for $p \leq p_c$ $P_\infty = 0$, whereas P_∞ is nonvanishing for $p > p_c$. Clearly $P_\infty = 1$ for $p = 1$. In general, every lattice site has two possibilities. It can be empty, with probability $1-p$, or it can be occupied, with probability p. If the site is occupied then there are again two possibilities. It can be an element of the percolating cluster, with probability pP_∞, or it is part of some finite cluster,

with probability $p(1-P_\infty)$. Note that

$$p(1-P_\infty)=\sum_s P_s \ , \tag{A3}$$

where $\sum_s$ denotes the sum over all finite clusters. Since the sum of these probabilities must be unity, it follows from (A2) and (A3) that

$$1-p+pP_\infty+\sum_s sn_s=1 \ . \tag{A4}$$

If the cluster numbers n_s are known, then P_∞ can be calculated from this expression. Hence the cluster numbers n_s are of fundamental importance.

The behavior of systems close to a phase transition is usually described by critical exponents. For percolation theory the relevant exponents are defined by

$$\begin{aligned}
\sum_s n_s(p)\Big|_{\text{sing}} &\propto |p-p_c|^{2-\alpha} \ , \\
\sum_s sn_s(p)\Big|_{\text{sing}} &\propto |p-p_c|^{\beta} \ , \\
\sum_s s^2 n_s(p)\Big|_{\text{sing}} &\propto |p-p_c|^{-\gamma} \ , \\
\sum_s sn_s(p)e^{-hs}\Big|_{\text{sing}} &\propto h^{1/\delta} \ ,
\end{aligned} \tag{A5}$$

where p is near p_c and h is near zero. The subscript "sing" denotes the leading nonanalytic part of the quantity and does not necessarily diverge as $p\to p_c$ or $h\to 0$. These critical exponents are not all independent as we will see below. Note that it follows from (A4) and (A5) that

$$P_\infty \propto (p-p_c)^\beta \tag{A6}$$

for p slightly above p_c. Otherwise P_∞ vanishes.

The cluster numbers n_s can be evaluated as follows. Fix s and consider one configuration of the s occupied lattice sites. Let t be the number of empty lattice sites that are nearest neighbors of the s occupied sites. These empty sites are called the perimeter of the configuration. Furthermore, let g_{st} be the number of configurations that are related to the above by a rotation. (Configurations that differ by a translation are considered to be equivalent.) Coefficient g_{st} counts the number of "animals" of type s and t. Now note that, in general, there are many different shape configurations of s occupied lattice sites, each with its own perimeter t and animal number g_{st}. It follows that the cluster number n_s is given by

$$n_s=\sum g_{st}p^s q^t \ , \tag{A7}$$

where $\sum$ is a sum over all different shape configurations. For very small s, n_s can readily be computed from this equation. However, as s increases the number of shapes and animals vastly increases and (A6) becomes useless. There is, however, a region of large s in which n_s can be computed by other means. This is in the so-called scaling regime in which $s\to\infty$ and $p\to p_c$. Define $z=(p-p_c)s^\sigma$ where σ is a parameter to be discussed below. Then, in the limit in which $s\to\infty$, $p\to p_c$, and z is finite,

$$n_s=q_0 s^{-\tau}f(z) \ , \tag{A8}$$

where τ is a second parameter independent of σ and f is a scaling function of z only with the property that

$$f(0)=1 \ . \tag{A9}$$

The form of f can be calculated in various ways and is dependent upon the dimension d. Similarly, constant q_0 can be computed and depends on d. Inserting (A8) into (A5) leads to the relations

$$\begin{aligned}
2-\alpha &= (\tau-1)/\sigma \ , \\
\beta &= (\tau-2)/\sigma \ , \\
-\gamma &= (\tau-3)/\sigma \ , \\
1/\delta &= \tau-2 \ .
\end{aligned} \tag{A10}$$

It follows that the critical exponents are not all independent and satisfy the equations

$$\begin{aligned}
\tau &= 2+1/\delta \ , \\
\sigma &= 1/\beta\delta = 1/(\gamma+\beta) \ , \\
2-\sigma &= \gamma+2\beta=\beta(\delta+1) \ .
\end{aligned} \tag{A11}$$

TABLE IV. The exact values of the cluster numbers $n_s(p)$ computed in $d=2$ on a square lattice for a range of values of p and small values of s. These were computed by explicit animal calculations.

p \ s	1	2	3	4	5	6	7	8
26	780×10^{-4}	222×10^{-4}	117×10^{-4}	658×10^{-5}	391×10^{-5}	241×10^{-5}	153×10^{-5}	998×10^{-6}
30	720×10^{-4}	212×10^{-4}	120×10^{-4}	728×10^{-5}	467×10^{-5}	311×10^{-5}	214×10^{-5}	151×10^{-5}
34	645×10^{-4}	191×10^{-4}	114×10^{-4}	729×10^{-5}	494×10^{-5}	349×10^{-5}	254×10^{-5}	190×10^{-5}
38	562×10^{-4}	164×10^{-4}	101×10^{-4}	671×10^{-5}	473×10^{-5}	347×10^{-5}	263×10^{-5}	206×10^{-5}
42	475×10^{-4}	134×10^{-4}	844×10^{-5}	570×10^{-5}	411×10^{-5}	309×10^{-5}	241×10^{-5}	193×10^{-5}
46	391×10^{-4}	105×10^{-4}	662×10^{-5}	450×10^{-5}	328×10^{-5}	249×10^{-5}	197×10^{-5}	160×10^{-5}
50	313×10^{-4}	781×10^{-5}	488×10^{-5}	330×10^{-5}	240×10^{-5}	182×10^{-5}	144×10^{-5}	117×10^{-5}
55	226×10^{-4}	502×10^{-5}	305×10^{-5}	200×10^{-5}	143×10^{-5}	106×10^{-5}	827×10^{-6}	665×10^{-6}
59	167×10^{-4}	331×10^{-5}	193×10^{-5}	122×10^{-5}	844×10^{-6}	610×10^{-6}	464×10^{-6}	365×10^{-6}
60	154×10^{-4}	295×10^{-5}	170×10^{-5}	106×10^{-5}	729×10^{-6}	522×10^{-6}	394×10^{-6}	307×10^{-6}
65	975×10^{-5}	155×10^{-5}	830×10^{-6}	484×10^{-6}	313×10^{-6}	211×10^{-6}	151×10^{-6}	112×10^{-6}
70	567×10^{-5}	714×10^{-6}	345×10^{-6}	182×10^{-6}	109×10^{-6}	675×10^{-7}	450×10^{-7}	313×10^{-7}

In other regimes of s and p the exact functional structure of n_s is unknown but there is some partial information. For example, in the regime $s \to \infty$, fixed p, it is known that

$$\ln n_s \propto -s^{\zeta} , \tag{A12}$$

where

$$\begin{aligned} \zeta(0 \le p < p_c) &= 1 , \\ \zeta(p_c < p \le 1) &= 1 - 1/d . \end{aligned} \tag{A13}$$

When $p = p_c$, the large-s behavior is described by (A8) and (A9).

Consider a fixed value of s and a specific configuration of s nearest neighbor connected occupied lattice sites. The radius of gyration of this configuration is defined by

$$\tilde{R}_s = \left(\sum_{i=1}^{s} |\vec{r}_i - \vec{r}_{\text{c.m.}}|^2 / s \right)^{1/2} , \tag{A14}$$

where $\vec{r}_i$ is the vector location of the ith occupied site and $\vec{r}_{\text{c.m.}}$ is the location of the center of mass of these sites. In general, different configurations of s occupied sites will have different radii of gyrations. One defines the radius of an s cluster, R_s, to be the animal weighted average over all possible configurations of s occupied sites. That is,

$$R_s = \left(\frac{\sum (g_{st} p^s q^t \tilde{R}_s^2)}{n_s} \right)^{1/2} , \tag{A15}$$

where $\sum$ is a sum over all different shape configurations. It is important to note that, in general, R_s is a function of p. As was the case for cluster numbers n_s, (A15) can be used to evaluate R_s for small values of s but rapidly becomes intractable as s increases. However, as was the case for n_s, R_s can be evaluated in the scaling regime where $s \to \infty$, $p \to p_c$, and $z = (p - p_c)s^{\sigma}$ is finite. In this limit

$$R_s = c_0 s^{\sigma\nu} R(z) , \tag{A16}$$

where ν is related to the previous critical exponents by

$$\nu d = \beta + \frac{1}{\sigma} \tag{A17}$$

and $R(z)$ is a scaling function of z only with the property

$$R(0) = 1 . \tag{A18}$$

$R(z)$ is known, and is given by

$$R(z) = |z|^{\beta\delta\varphi - \nu} , \tag{A19}$$

where the value of φ depends on the regime of p. For $p = p_c$, z vanishes and (A18) requires that

$$\varphi(p = p_c) = \nu / \beta\delta . \tag{A20}$$

For $p > p_c$ it is known that

$$\varphi(p > p_c) = 1/d . \tag{A21}$$

Finally, for $p < p_c$ there are rough theoretical estimates for φ which are not consistent with Monte Carlo data. It is safest to use the Monte Carlo results which depend on d. Finally, constant c_0 can be computed and is d dependent. Combining (A16) and (A19) we find that, in the scaling regime,

$$R_s = c_0 |p - p_c|^{\beta\delta\varphi - \nu} s^{\varphi} . \tag{A22}$$

The percolation correlation length ζ is defined as a weighted average over R_s given by

$$\zeta = \left(\frac{\sum_s s^2 n_s R_s^2}{\sum s^2 n_s} \right)^{1/2} . \tag{A23}$$

It can be shown that, as $p \to p_c$,

$$\zeta \propto |p - p_c|^{-\nu} . \tag{A24}$$

Note that ζ is a function of p. It is very hard to compute ζ directly from Eq. (A23). However, there is a procedure that allows one to get a fairly accurate expression for ζ. If one examines the explicit structure of the scaling function f in (A8), one discovers that f is approximately constant for $z < z_\zeta$, where z_ζ is some computable value, and f decays exponentially as z^2 for $z > z_\zeta$. Furthermore, z_ζ is found to be close to p_c. It follows that z_ζ corresponds

TABLE IV. (*Continued*)

9	10	11	12	13	14	15	16	17
660×10^{-6}	443×10^{-6}	300×10^{-6}	206×10^{-6}	142×10^{-6}	984×10^{-7}	687×10^{-7}	481×10^{-7}	339×10^{-7}
108×10^{-5}	787×10^{-6}	579×10^{-6}	430×10^{-6}	321×10^{-6}	242×10^{-6}	183×10^{-6}	140×10^{-6}	107×10^{-6}
145×10^{-5}	112×10^{-5}	873×10^{-6}	689×10^{-6}	548×10^{-6}	439×10^{-6}	354×10^{-6}	287×10^{-6}	233×10^{-6}
163×10^{-5}	131×10^{-5}	107×10^{-5}	886×10^{-6}	738×10^{-6}	618×10^{-6}	522×10^{-6}	443×10^{-6}	377×10^{-6}
158×10^{-5}	131×10^{-5}	110×10^{-5}	938×10^{-6}	805×10^{-6}	696×10^{-6}	606×10^{-6}	530×10^{-6}	467×10^{-6}
133×10^{-5}	112×10^{-5}	959×10^{-6}	831×10^{-6}	726×10^{-6}	640×10^{-6}	568×10^{-6}	507×10^{-6}	456×10^{-6}
975×10^{-6}	825×10^{-6}	712×10^{-6}	621×10^{-6}	547×10^{-6}	485×10^{-6}	434×10^{-6}	391×10^{-6}	354×10^{-6}
548×10^{-6}	461×10^{-6}	393×10^{-6}	341×10^{-6}	298×10^{-6}	263×10^{-6}	235×10^{-6}	211×10^{-6}	190×10^{-6}
294×10^{-6}	243×10^{-6}	204×10^{-6}	173×10^{-6}	149×10^{-6}	130×10^{-6}	114×10^{-6}	101×10^{-6}	901×10^{-7}
246×10^{-6}	201×10^{-6}	168×10^{-6}	142×10^{-6}	122×10^{-6}	106×10^{-6}	922×10^{-7}	812×10^{-7}	721×10^{-7}
861×10^{-7}	676×10^{-7}	541×10^{-7}	440×10^{-7}	363×10^{-7}	303×10^{-7}	256×10^{-7}	218×10^{-7}	187×10^{-7}
224×10^{-7}	165×10^{-7}	125×10^{-7}	959×10^{-8}	750×10^{-8}	594×10^{-8}	476×10^{-8}	386×10^{-8}	316×10^{-8}

to an s value given by

$$s_\zeta = \left(\frac{p_c}{|p - p_c|}\right)^{1/\sigma} . \tag{A25}$$

Substituting this expression into (A22) gives

$$R_{s_\zeta} = c_0 (p_c)^{\delta\beta\varphi} |p - p_c|^{-\nu} , \tag{A26}$$

which has the appropriate scaling behavior for ζ. It turns out that setting

$$\zeta = R_{s_\zeta} \tag{A27}$$

is a very good approximation to ζ. Note that (since ν is positive) for p away from p_c, ζ is small, whereas $\zeta \to \infty$ at $p \to p_c$, as it must.

Consider some value of p with ζ the associated correlation length. For any finite s cluster with the property that $R_s \ll \zeta$ or $R_s \gg \zeta$ it can be shown that

$$s = A R_s^D , \tag{A28}$$

where D is the "fractal" dimension (in general, different than d), A is a function of p, and both D and A depend on the regime of p. First consider the $p = p_c$ regime. In this case $\zeta \to \infty$ and $R_s \ll \zeta$ for any finite s. Such systems are "self-similar," from which it can be proven that

$$D(p = p_c) = \frac{d}{1 + 1/\delta} . \tag{A29}$$

Recall that for $p = p_c$ in the scaling regime

$$R_s = c_0 s^{\nu/\beta\delta} . \tag{A30}$$

Inserting (A29) and (A30) into (A28) gives

$$s = (\bar{A} c_0^{d/(1+1/\delta)}) s^{\nu d/(1+1/\delta)\beta\delta} , \tag{A31}$$

where $\bar{A}$ denotes the parameter A at $p = p_c$. Consistency requires that

$$\nu d = (1 + 1/\delta)\beta\delta \tag{A32}$$

which, using (A11) and (A17), is easily shown to be true. Furthermore, we must have

$$c_0 = \bar{A}^{-d/(1+1/\delta)} , \tag{A33}$$

which allows us to find c_0 from existing Monte Carlo data on fractals at $p = p_c$. We further conclude that, since (A28) is valid for all s when $p = p_c$, Eq. (A30) is also valid for all s, not just the $s \to \infty$ scaling regime. Now consider the case that $p \neq p_c$ but s is such that $R_s \ll \zeta$. It is clear that, for such small clusters, R_s is still given by (A30) and the fractal dimensions by (A29). We can invert the logic of the previous discussion to derive a general expression for the fractal dimension in terms of the parameter φ. Inserting (A22) into (A28) yields the conditions

$$D = 1/\varphi \tag{A34}$$

TABLE V. The exact values of the cluster numbers $n_s(p)$ computed in $d = 3$ on a simple cubic lattice for a range of values of p and small values of s. These were computed by explicit animal calculations.

p \ s	1	2	3	4	5	6	7	8	9	10	11
10	531×10^{-3}	105×10^{-3}	373×10^{-4}	156×10^{-4}	709×10^{-5}	341×10^{-5}	170×10^{-5}	874×10^{-6}	459×10^{-6}	246×10^{-6}	133×10^{-6}
15	377×10^{-3}	886×10^{-3}	396×10^{-4}	208×10^{-4}	120×10^{-4}	738×10^{-5}	471×10^{-5}	309×10^{-5}	208×10^{-5}	142×10^{-5}	991×10^{-6}
20	262×10^{-3}	644×10^{-4}	317×10^{-4}	185×10^{-4}	120×10^{-4}	826×10^{-5}	593×10^{-5}	140×10^{-5}	331×10^{-5}	259×10^{-5}	204×10^{-5}
25	178×10^{-3}	422×10^{-4}	212×10^{-4}	127×10^{-4}	859×10^{-5}	617×10^{-5}	164×10^{-5}	361×10^{-5}	288×10^{-5}	235×10^{-5}	194×10^{-5}
30	118×10^{-3}	254×10^{-4}	123×10^{-4}	724×10^{-5}	482×10^{-5}	344×10^{-5}	257×10^{-5}	200×10^{-5}	159×10^{-5}	130×10^{-5}	108×10^{-5}
31	108×10^{-3}	227×10^{-4}	109×10^{-4}	634×10^{-5}	418×10^{-5}	297×10^{-5}	221×10^{-5}	170×10^{-5}	135×10^{-5}	110×10^{-5}	909×10^{-6}
35	754×10^{-4}	141×10^{-4}	632×10^{-5}	349×10^{-5}	220×10^{-5}	150×10^{-5}	107×10^{-5}	800×10^{-6}	615×10^{-6}	183×10^{-6}	388×10^{-6}
10	467×10^{-4}	726×10^{-5}	288×10^{-5}	144×10^{-5}	832×10^{-6}	522×10^{-6}	317×10^{-6}	240×10^{-6}	172×10^{-6}	126×10^{-6}	949×10^{-7}
45	277×10^{-4}	312×10^{-5}	116×10^{-5}	509×10^{-6}	261×10^{-6}	116×10^{-6}	873×10^{-7}	546×10^{-7}	354×10^{-7}	236×10^{-7}	162×10^{-7}
50	156×10^{-4}	146×10^{-5}	412×10^{-6}	152×10^{-6}	669×10^{-7}	325×10^{-7}	170×10^{-7}	93×10^{-7}	53×10^{-7}	31×10^{-7}	19×10^{-7}

and

$$A = \left(\bar{A}^{d/(1+1/\delta)}|p-p_c|^{\nu-\beta\delta\varphi}\right)^{1/\varphi} . \quad \text{(A35)}$$

For $p = p_c$ or $p \neq p_c$ and $R_s \ll \zeta$ (A34) and (A35) give (A29) and $A = \bar{A}$, respectively. For $p > p_c$ and $R_s \gg \zeta$, it follows from (A21) and (A34) that

$$D(p > p_c) = d . \quad \text{(A36)}$$

Therefore on this regime

$$A = \bar{A}^{d^2/(1+1/\delta)}|p-p_c|^{\beta} , \quad \text{(A37)}$$

where we have used expression (A32). Finally, for $p < p_c$ and $R_s \gg \zeta$, Eqs. (A34) and (A35) determine D and A given the Monte Carlo value for φ in this regime.

The above considerations can be used to derive an expression for P_∞ for p near to p_c. Assume $p > p_c$. Then for $s \to \infty$, the density of occupied points is well approximated by pP_∞. It follows that, in d dimensions, for $s \to \infty$,

$$s = pP_\infty \frac{\pi^{d/2}}{\Gamma(d/2+1)} R_s^d . \quad \text{(A38)}$$

Inserting expression (A22) for R_s into (A38) and using (A21) and (A32) we find

$$P_\infty = \frac{\Gamma(d/2+1)}{\pi^{d/2} c_0^d} \frac{1}{p} |p-p_c|^{\beta} . \quad \text{(A39)}$$

Note that this expression is only valid for $p - p_c$ positive and small and is of the form given in (A6).

Fix s and consider one configuration of s occupied lattice sites with t empty nearest neighbor sites. Assume the number of animals of this type is g_{st}. Then one defines the average perimeter of an s cluster of any type to be

$$t_s = \frac{\sum (g_{st} p^s q^t t)}{n_s} , \quad \text{(A40)}$$

where $\sum$ is a sum over all different shape configurations. Note that t_s is, in general, a function of p. It is not hard to show that

$$t_s = \left(\frac{1-p}{p}\right) s - (1-p)\frac{\partial}{\partial p} \ln n_s . \quad \text{(A41)}$$

Recall that the structure of a d-dimensional lattice is not unique. It is important to ask which of the percolation quantities defined above are "universal," that is, independent of lattice structures, and which quantities are not. It turns out that the critical exponents $\alpha, \beta, \gamma, \delta, \nu$ and $\sigma, \tau, \zeta, \varphi$ are universal. Furthermore, the scaling functions $f(z)$ and $R(z)$ are found to be universal. We emphasize that these universal quantities can and do depend on the dimension d. An important quantity which is not universal is the value of p_c, which exhibits a mild dependency on the lattice structure. Two other nonuniversal quantities are q_0 and c_0 which again depend weakly on the structure of the lattice.

APPENDIX B: CLUSTER NUMBERS

In this appendix we list the cluster numbers $n_s(p)$ for a range of values of s and p in both two and three dimensions. These results were first obtained from direct animal calculations in the two references in [14]. We reproduce their results in this appendix since they are vital to the discussions of the range of the scaling approximations to $n_s(p)$ given in Secs. II and III. The values of $n_s(p)$ computed on a square lattice in $d = 2$, for a set of p's between 26 and 70 and for $1 \leq s \leq 17$, are listed in Table IV. The values of $n_s(p)$ computed on a simple cubic lattice in $d = 3$, for a set of p's between 10 and 50 and for $1 \leq s \leq 11$, are listed in Table V.

[1] G. Abell, Astrophys. J. Suppl. **3**, 211 (1958).
[2] N. A. Bahcall, Astrophys. J. **232**, 689 (1979).
[3] V. de Lapparent, M. J. Geller, and J. Huchra, Astrophys. J. **302**, L1 (1986).
[4] A. Guth and S. Y. Pi, Phys. Rev. Lett. **49**, 1110 (1982); A. A. Starobinskii, Phys. Lett. **117B**, 179 (1982); S. W. Hawking, *ibid.* **115B**, 295 (1982); J. M. Bardeen, P. J. Steinhardt, and M. S. Turner, Phys. Rev. D **28**, (1983).
[5] Ya. B. Zeldovich, I. Yu. Kobzarev, and L. B. Okun, Sov. Phys. JETP **40**, 1 (1975), and references therein.
[6] A. Albrecht and N. Turok, Phys. Rev. Lett. **54**, 1868 (1985); R. Brandenberger and N. Turok, Phys. Rev. D **33**, 2175 (1986), and references therein.
[7] D. Spergel and N. Turok, Phys. Rev. Lett. **64**, 2736 (1990); Phys. Rev. D **43**, 1038 (1991).
[8] I. Wasserman, Phys. Rev. Lett. **57**, 2234 (1986); C. Hill, D. Schramm, and J. Fry, Comments Nucl. Part. Phys. **19**, 25 (1989); C. Hill, D. Schramm, and D. Widrow, Report No. Fermilab-PUB-89/166-T, 1989 (unpublished).
[9] C. Hill and G. Ross, Nucl. Phys. **B311**, 253 (1988); Phys. Lett. B **203**, 125 (1988); A. Gupta, C. Hill, R. Holman, and E. Kolb, Phys. Rev. D **45**, 441 (1992); J. Frieman, C. Hill, and R. Watkins, *ibid.* **46**, 1226 (1994).
[10] B. Ovrut and S. Thomas, Phys. Lett. B **277**, 53 (1992); **257**, 292 (1991); **267**, 227 (1991).
[11] W. Press, B. Ryden, and D. Spergel, Astrophys. J. **347**, 590 (1989).
[12] For reviews, see D. Stauffer, Phys. Rep. **54**, 1 (1979); A. Aharony, in *Directions in Condensed Matter Physics*, edited by G. Grinstein and G. Mazenko (World Scientific, Singapore, 1986).
[13] M. Sykes, D. Gaunt, and M. Glen, J. Phys. A **9**, 1705 (1976); A. Flammang, Z. Phys. B **28**, 47 (1977).
[14] J. Hoshen *et al.*, J. Phys. A **12**, 1285 (1979); also see H. Nakaniski and H. E. Stanley, Phys. Rev. B **22**, 2466 (1980).
[15] D. Stauffer, Z. Phys. B **30**, 173 (1978).
[16] H. P. Peters, D. Stauffer, H. P. Hölters, and K. Loewenich, Z. Phys. B **34**, 399 (1979).
[17] D. Stauffer, *Introduction to Percolation Theory* (Taylor & Francis, London, 1985).
[18] A. Linde, *Particle Physics and Inflationary Cosmology*

(Harwood-Academic, Chur, Switzerland, 1990), Chap. 7; A. Linde and D. H. Lyth, Phys. Lett. B **246**, 353 (1990).
[19] E. Kolb and Y. Wang, Phys. Rev. D **45**, 4421 (1992); G. Gelmini, M. Gleiser, and E. Kolb, *ibid.* **39**, 1558 (1989).
[20] Z. Lalak and B. A. Ovrut, Phys. Rev. Lett. **71**, 951 (1993).
[21] Z. Lalak, S. Lola, B. A. Ovrut, and G. G. Ross, Nucl. Phys. **B434**, 675 (1995).
[22] P. J. E. Peebles, *The Large Scale Structure of the Universe* (Princeton University Press, Princeton, NJ, 1980).
[23] A. Stebbins and M. S. Turner, Astrophys. J. Lett. **339**, L13 (1991); G. Goetz and D. Notzold, Nucl. Phys. **B351**, 645 (1991).